STUDIA UNIVERSITATIS BABEŞ-BOLYAI, CHEMIA, LII, 3, 2007

AMINO ACIDS BINDING TO GOLD NANOPARTICLES

OSSI HOROVITZ[a], AURORA MOCANU[a], GHEORGHE TOMOAIA[b], MARIA CRISAN[c], LIVIU-DOREL BOBOS[a], CSABA RACZ[a] AND MARIA TOMOAIA-COTISEL[a]

ABSTRACT. Gold nanoparticles capped with citrate anions were synthesized and characterized by UV-Vis spectroscopy; a strong absorption is identified at about 528 nm, corresponding to the surface plasmon resonance (SPR). The gold nanoparticles were analyzed by transmission electron microscopy (TEM) and TEM images indicate a mean gold nanoparticle size of 14 nm. The colloidal gold aqueous solution is stable in time, indicating a good electrostatic stabilization of gold nanoparticles through the adsorbed monolayer of citrate anions on gold nanoparticle surface. The interaction between the citrate capped gold nanoparticles in aqueous solution and various amino acids was investigated monitoring their UV-Vis spectra. Some of the tested amino acids, like glycine, isoleucine and asparagine, showed little interaction with gold nanoparticles. However, other amino acids, such as lysine, arginine, glutamic acid, histidine, cysteine and methionine, presented an absorption decrease of the colloidal gold solution at 528 nm and a bathochromic shift of the absorption maximum. At higher amino acid:gold molar ratios a new, large absorption band appears in the range of 600 to 700 nm, which increases in time. As a consequence of the assembly formation of gold nanoparticles, the color of the colloidal gold solution changes from red to blue. Further, TEM and atomic force microscopy (AFM) images evidenced the arrangements of gold nanoparticles mediated by amino acids. The analysis of AFM images indicate a close packed and an almost equidistant arrangement of gold nanoparticles coated by amino acids, especially for cysteine, arginine and lysine. These arrangements indicate a stabilization effect, mediated by these amino acids bonded to gold nanoparticle surface.

INTRODUCTION

There is increased current interest in the area of nanotechnology due to the outstanding physical and chemical properties of nanoparticles with potential applications in optoelectronic devices, non-linear optics and biosensors, just to name a few. One of the aims in nanotechnology is the organization of nanoparticles in thin films with the ability to modify and control the size and separation as well as the interactions between particles.

[a] Babeş-Bolyai University of Cluj-Napoca, Faculty of Chemistry and Chemical Engineering, Arany J. Str., no 11, 400028 Cluj-Napoca, Romania
[b] Iuliu Haţieganu University of Medicine and Pharmacy, Department of Orthopedic Surgery, Mosoiu Str., no. 47, 400132 Cluj-Napoca, Romania
[c] Iuliu Haţieganu University of Medicine and Pharmacy, Department of Histology, Clinic of Dermatology, Clinicilor Str., no. 3, 400006 Cluj-Napoca, Romania;
e-mail: horovitz@chem.ubbcluj.ro, mcotisel@yahoo.com

Consequently, the optical and electronic properties of these assemblies can be tailored. Strategies are developed and explored for assembling metallic nanoparticles and biological molecules, in order to develop new materials for electronics and optics, and for biomedical and bioanalytical areas, such as controlled drug delivery, medical diagnosis and biosensors [1-6].

Among biological molecules, amino acids are important organic compounds to be used in biofunctionalization of gold nanoparticles, as protective layers and for their assembly in thin films. Functional groups such as -SH and $–NH_2$ present a high affinity for gold, and since amino acids contain some of these groups, they are expected to stabilize gold nanoparticles. Their capacity of generating structural diversity was recognized [7], and gold surfaces capped with amino acids are considered to represent the simplest models for protein surfaces [8].

There are relatively few reports on surface modifications of gold nanoparticles with amino acid molecules, and no systematic study of amino acid interactions with gold nanoparticles is available [9]. The binding of cysteine and lysine to gold nanoparticles was reported [10], and a review on amino acid interactions with metallic nanoparticles was given [11]. Some amino acids were used as reduction and capping agents for silver or gold nanoparticles, e.g. lysine [12-14], tryptophan [14, 15], aspartic acid [13, 16], tyrosine [14, 17], arginine [14, 17], cysteine, leucine and asparagine [18], and also the dipeptide glycyl-tyrosine [17]. The S-Au interaction in cysteine capped gold nanoparticels was discussed [18-21] and the binding of cysteine to Au was compared with that of leucine and asparagine [20]. Gold-silver nanocomposites were prepared from gold nanorod seeds in amino acid solutions: arginine, cysteine, glycine, glutamine, glutamate, histidine, lysine, and methionine [22].

Amino acids can be adsorbed on the particle surface already during the formation of particles, using the amino acid itself as reduction agent [14-18], or in a latter stage, by ligand exchange reactions or binding on the former adsorbed stabilizing molecules. In this way homogeneous monolayers or heterogeneous, mixed layers can be obtained. A pentapeptide was also used as a ligand on gold nanoparticles [23]. Cysteine adsorbed on a gold surface was used to immobilize protein molecules [24-26].

Previously, we have focused on the synthesis and physicochemical properties of citrate anions capped gold nanoparticles and on their organization in thin films on hydrophobic glass plates [27-30]. Surface functionalization of gold nanoparticles has been accomplished using a globular protein, extracted from aleurone cells of barley [27]. How citrate anions, capping agents of gold nanoparticles, are involved in the interaction between surface-modified gold nanoparticles and proteins is an important

question to be answered. An answer can be obtained by a systematic study of amino acids binding to gold nanoparticles.

This work is a follow-up to our ongoing research projects on the binding of amino acids and peptides to the gold colloidal nanoparticles. It deals with the synthesis of gold nanoparticles of controlled size and shape and with the functionalization of gold particles with different organic molecules, e.g. nine amino acids and two peptides. The interaction between gold nanoparticles and said organic molecules is observed by UV-Vis spectroscopy. Further, the deposition and organization of gold nanoparticle assemblies, in the presence of cysteine, arginine and lysine, are investigated by TEM and AFM.

EXPERIMENTAL PART

Materials

A colloidal gold solution was prepared by $HAuCl_4$ reduction with sodium citrate, in a variant of the Turkevich method, as adapted from [31]. The tetrachloroauric (III) acid was purchased from Merck (high purity above 99.5 %). The trisodium citrate dihydrate ($Na_3C_6H_5O_7 \cdot 2H_2O$) was obtained from Sigma Aldrich (high purity above 99%). All chemicals were used without further purification. Deionized water with resistivity of 18 MΩ·cm was used in all experiments and it was obtained from an Elgastat water purification system. 200 mL 0.005% (w/w) $HAuCl_4 \cdot 3H_2O$ solution stirred vigorously was refluxed. To the boiling solution 15.3 mg trisodium citrate ($Na_3C_6H_5O_7 \cdot 2H_2O$), solved in a minimum amount of water, was added. After colour change, the heat was turned off and the solution was allowed to cool overnight to room temperature. The gold content in the final colloidal solution is 25 mg/L. The resulting solution of colloidal gold particles was stored in a brown bottle and kept at 4 ^oC.

The solid L-amino acids were purchased from Sigma and used without further purification. They were dissolved in deionized water. The amino acids used in this investigation, their three letter code, one letter code and the concentrations of their solutions (put in parentheses, in mol/L) were the following: L-glycine, Gly, G (0.41); L-isoleucine, Ile, I (0.1); L-glutamic acid, Glu, E (0.1); L-asparagine. Asn, N (0.5 M); L-cysteine, Cys, C (0.001; 0.01; 0.1); L-methionine, Met, M (0.2; 0.4); L-lysine, Lys, K (0.01; 0.1; 0.54); L-arginine, Arg, R (0.01; 0.1); L-histidine, His, H (0.01; 0.1).

Methods

The UV/VIS absorption spectrum of the solutions was studied using a Jasco UV/VIS V-530 spectrophotometer with 10 mm path length quartz cuvettes in the 190 – 900 nm wavelengths range.

The investigated mixtures were obtained from the gold colloidal solution (c_{Au}) and the amino acid solutions (concentration c_{AA}), by successive removal of

small amounts of the previous mixture and adding of equal amounts of amino acid solution. The gold and amino acid contents in the resulting mixtures and their ratios, used in most of the determinations, are given in Table 1.

Table 1.

Gold: amino acid ratios in the investigated mixtures. (c_{Au} = concentration of the gold colloidal solution; c_{AA} = concentration of the amino acid solution)

Gold content reported to c_{Au}	Amino acid content reported to c_{AA}	Content Au : AA ratio reported to (c_{Au}/c_{AA})
0.833	0.167	5 / 1
0.695	0.305	2.2 / 1
0.579	0.421	1.4 / 1
0.482	0.518	1 / 1.1
0.402	0.598	1 / 1.5
0.335	0.665	1 / 2
0.321	0.679	1 /2.1
0.214	0.786	1 / 3.7

The colloidal gold nanoparticles suspension in the absence and in the presence of amino acids was deposited and air dried on the specimen grid and observed with a transmission electron microscope (TEM: JEOL – JEM 1010). TEM specimens consist of carbon or collodion coated copper grids. TEM images were recorded with a JEOL standard software.

Atomic force microscopy (AFM) investigations were executed on the gold nanostructured films made from gold nanoparticles functionalized with amino acids using a commercial AFM JEOL 4210 equipment with a 10 x 10 (x-y) μm scanner operating in tapping (noted *ac*) mode [32-34]. Standard cantilevers, non-contact conical shaped of silicon nitride coated with aluminum, were used. The tip was on a cantilever with a resonant frequency in the range of 200 - 300 kHz and with a spring constant of 17.5 N/m. AFM observations were repeated on different areas from 30 x 30 μm^2 to 250 x 250 nm^2 of the same gold film. The images were obtained from at least ten macroscopically separated areas on each sample. All images were processed using the standard procedures for AFM. The sizes of nanoparticles were measured directly from AFM 2D-topographic images and their 3D-views. The thickness (vertical distance) variations were estimated from vertical linear cross sections and height distributions on AFM images [32-34]. AFM images consist of multiple scans displaced laterally from each other in y direction with 512 x 512 pixels. Low pass filtering was performed to remove the statistical noise without to loose the features of the sample. All AFM experiments were carried out under ambient laboratory conditions (about 20 ^oC) as previously reported [34].

RESULTS AND DISCUSSION

Characterization of the colloidal gold solution

The visible absorption spectra of the gold colloidal aqueous solution presents a well-defined absorption band with a maximum at the wavelength λ_{max} = 527 – 528 nm. This value is characteristic for plasmon absorbance for nanometric Au particles. The wavelength was not significantly modified, during a year after preparation, thus suggesting the stability of the colloidal solution.

The size of the gold colloid particles has been measured by TEM imaging. Two representative TEM images of these particles are given in Fig.1. The particles show mostly spherical or elliptical shape, just a few triangles, pentagons or hexagons are observed. From the sizes of a great number of particles, measured on the TEM images, an average size (diameter) of 14.2 nm with a standard deviation of 2.6 were calculated as well as the extreme values of the sizes, from 8.5 to 24 nm. From the average size, the approximate average mass of a particle (considered spherical) is estimated as $2.9 \cdot 10^{-17}$ g, the number of gold atoms in a particle

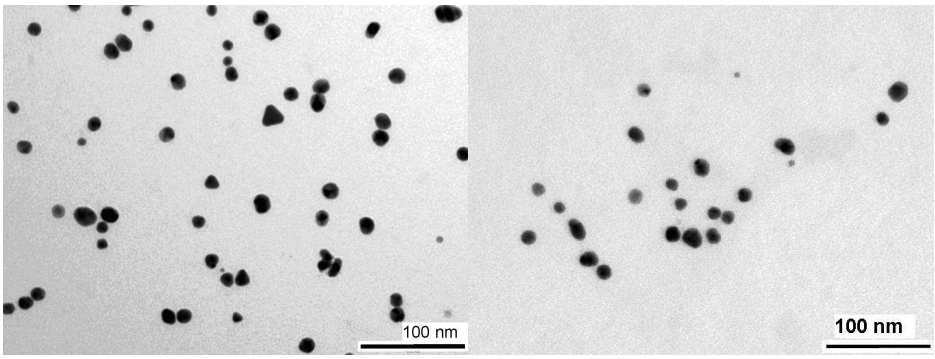

Fig.1. TEM images of gold nanoparticles

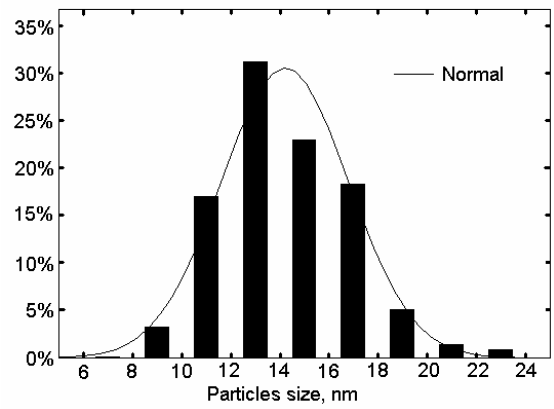

Fig.2. Histogram of size distribution for gold particles

is $8.8 \cdot 10^4$ and the number of particles per cm^3 of solution is $8.6 \cdot 10^{11}$. The histogram providing the size distribution of gold nanoparticles, obtained from TEM images is given in Figure 2. For comparison, the curve indicating the expected normal distribution was added.

The colloidal gold solution proved as very stable in time, without observable modifications in the UV-Vis spectrum for a year after preparation. This indicates electrostatic stabilization via citrate anions bonded on the gold nanoparticle surface. Therefore, the citrate capped gold nanoparticles are negatively charged.

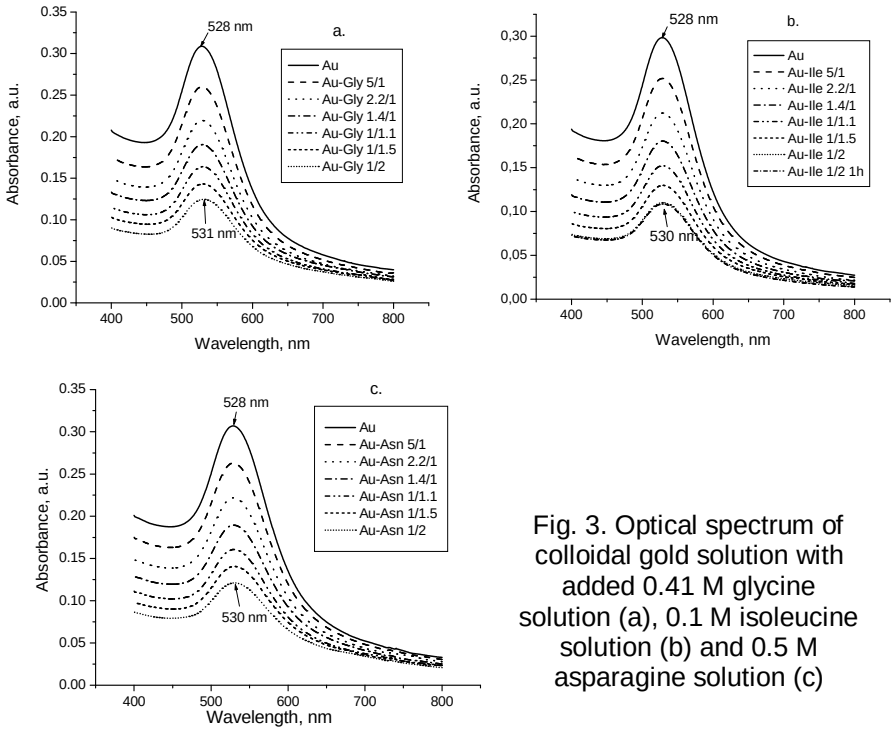

Fig. 3. Optical spectrum of colloidal gold solution with added 0.41 M glycine solution (a), 0.1 M isoleucine solution (b) and 0.5 M asparagine solution (c)

Interactions with amino acid solutions

The ***UV-Vis spectra*** of the amino acids present no adsorption bands in the range of wavelengths investigated here. For instance, the absorption maximum for arginine lies at 194 nm, for glycine under 190 nm, methionine presents a shoulder at 198 nm.

Adding of some of the amino acids produces no or little modification in the UV-Vis spectra of the gold colloidal solution. Besides the lowering of the absorbance due to the dilution of the gold solution, the absorption maxima are lightly shifted towards longer wavelength. This shift is due to

the change in the dielectric constant in the adsorption layer, the increase of the average refractive index of the environment surrounding the nanoparticles, and to the size increase of particles by the adsorbed layer [3]. For a *glycine* solution the maximum shift was 3 nm (Fig.3a), for an *isoleucine* solution 2 nm (Fig. 3b) and the same shift is observed for the *asparagine* solution (Fig. 3c). The shift does not change in time, i.e. the gold solutions with added amino acids remain stable in time (see, for instance Fig. 3b). We can assume the zwitterionic amino acid molecules to be settled by the $–NH_3^+$ group on the negative charged gold nanoparticle surface, while their $–COO^-$ group contributes further to the negative surface charge of the nanoparticles.

By adding the 0.2 M and 0.4 M *methionine* solution there are also only small shifts in the absorption maximum, but after four days a second absorption band appears at higher wavelengths, partially overlapped with the initial absorption band, with a shoulder at about 620 nm (Figs. 4a, b). For a higher colloidal gold concentration, the second band is more distinct, with a peak at 618 nm (Fig.4c). The new band is characteristic for the aggregation of nanoparticles. As a matter of fact, it is known that the apparition of the broad peak at longer wavelengths in the UV-Vis spectrum comes from the coupling of surface plasmon resonance (SPR) of two adjacent nanoparticles and it is an indication of the anisotropic optical properties of the gold nanoparticles aggregates [35].

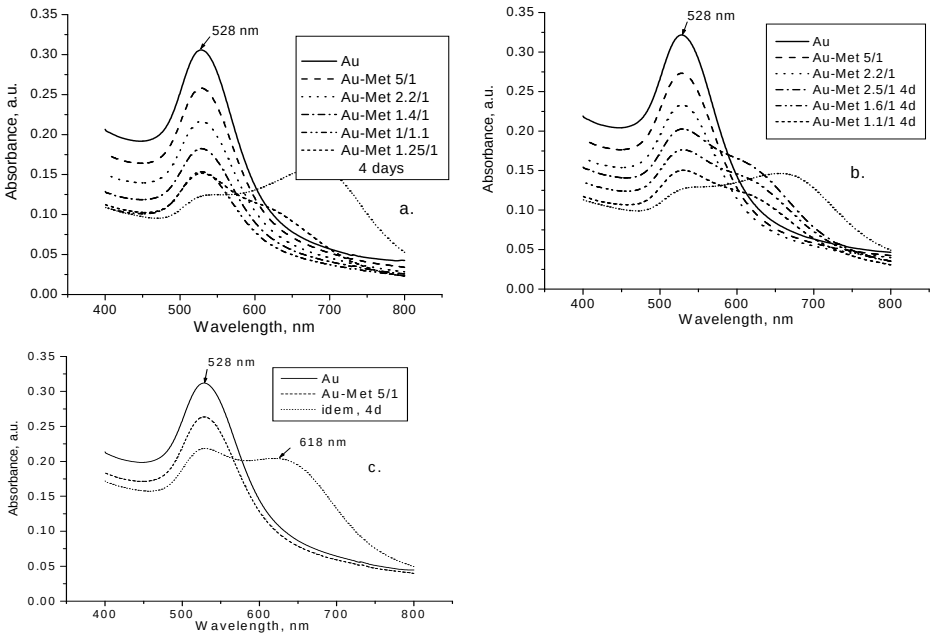

Fig.4. Optical spectrum of colloidal gold solution with added 0.2 M (a) and 0.4 M (b) methionine solution at different ratios and after 4 days, and for a higher gold content with 0.2 M methionine solution (c)

This tendency towards aggregation is much more pregnant when a sufficiently concentrated *lysine* solution is added (Fig.5). For a very diluted 0.01 M lysine solution (Fig. 5a) the plots look like those in Figure 3, with a small shift of the absorption band maximum. For a more concentrated 0.1 M solution (Fig. 5b) the shift towards higher wavelengths is much more important, and for higher quantities of lysine added the band becomes larger, suggesting an increasing aggregation of the nanoparticles. With a very concentrated (0.54 M) lysine solution, the band for aggregates appears at once (maximum at about 634 nm), while the 528 nm band for individual gold particles decreases and is observed only as a shoulder in the spectrum. The maximum of the broad absorption band continues its shift towards higher wavelengths in time (Fig. 5c). The color of the solution changed from reddish to blue. This kind of color change as an effect of aggregation is a well-understood phenomenon [36-38]. When the interparticle distance in the aggregates decreases to less than about the average particle diameter, the electric dipole–dipole interaction and coupling between the plasmons of neighboring particles in the aggregates results in the bathochromic shift of the absorption band. It has been used to study molecular recognition processes using gold nanoparticles in solution [39].

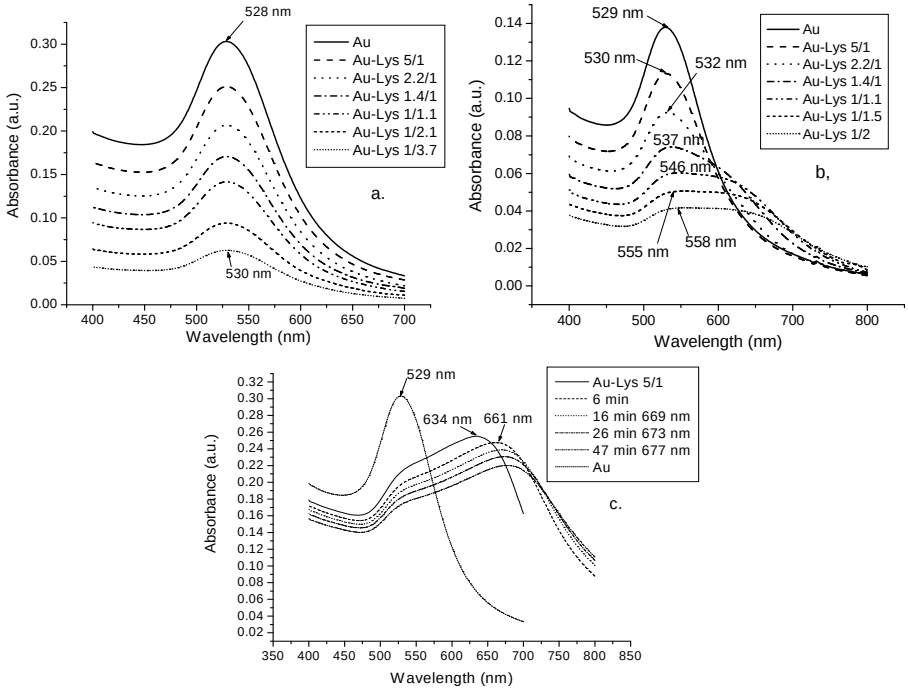

Fig.5. Optical spectrum of colloidal gold solution with added 0.01 M (a) and 0.1 M (b) lysine solution at different ratios, and with 0.54 M lysine solution in time (c)

Lysine adsorption on gold nanoparticles has been investigated [40], using 13 nm diameter gold particles and a $7 \cdot 10^{-4}$ M L-lysine solution at pH = 10.7. The UV-Vis spectrum showed a SPR peak at 520 nm, similar to that we found for citrate coated nanoparticles. The result is similar to our data, using the most diluted lysine solution (Fig. 5a). By adding a condensing agent, the authors [40] observed that particles aggregated by the formation of peptide bonds between two lysine molecules adsorbed on different nanoparticles. In the UV-Vis spectrum the SPR band of Au was shifted to 527 nm and a new broad peak appeared at 633 nm. The spectrum is similar to that obtained by us at high concentrations of the lysine solution.

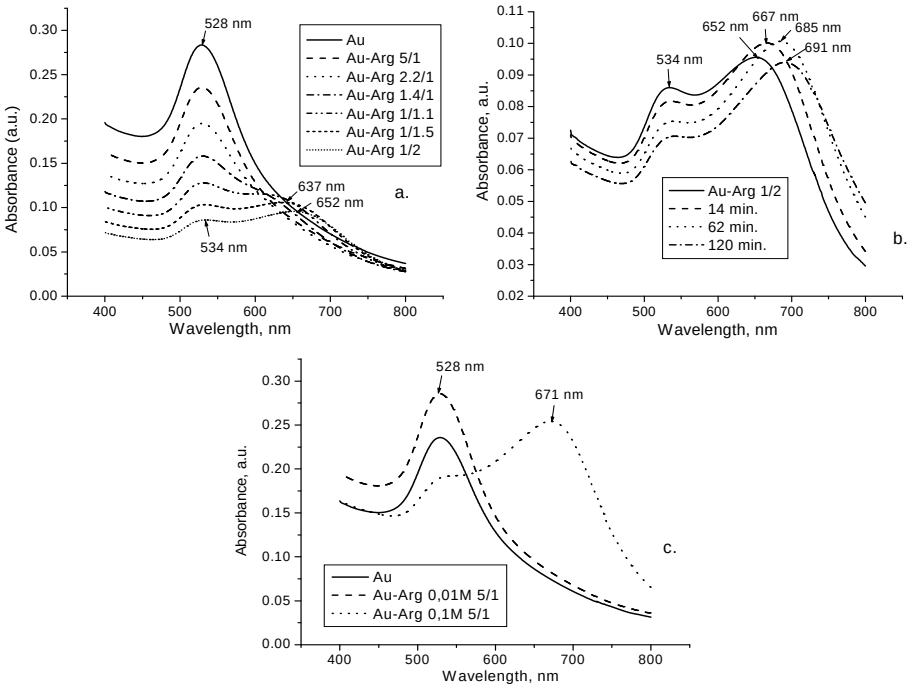

Fig.6. Optical spectrum of colloidal gold solution with 0.01 M arginine solution in different ratios (a) and time evolution (b) and with arginine solutions of different concentrations (c).

A similar behavior is observed in colloidal gold solutions with *arginine*. For a 0.01 M concentration of the arginine solutions and small added amounts, the maximum of the gold nanoparticles absorption is only slightly shifted, but at the 1.4:1 gold / arginine solution ratio the new band for particle aggregates appears, initially as a shoulder. By further adding arginine, the band broadens and its maximum shifts to 640-650 nm (Fig.6a). The time evolution of the aggregation is shown in Fig. 6b for the

colloidal Au / 0.01 M arginine solution ratio 1/2. The maximum is shifted further towards longer wavelengths. The adding of a more concentrated (0.1 M) arginine solution leads directly to the formation of the aggregates and to the colour change of the solution (Fig. 6c).

Likewise, a 0.01 M *histidine* solution leads to aggregation beyond a certain added quantity (Fig. 7a); the maxima of the new bands are in the wavelength range 670-690 nm. The 0.1 M histidine solution produces aggregation already at the first added amount (Fig. 7b); the maximum of the new band is found at about 700 nm.

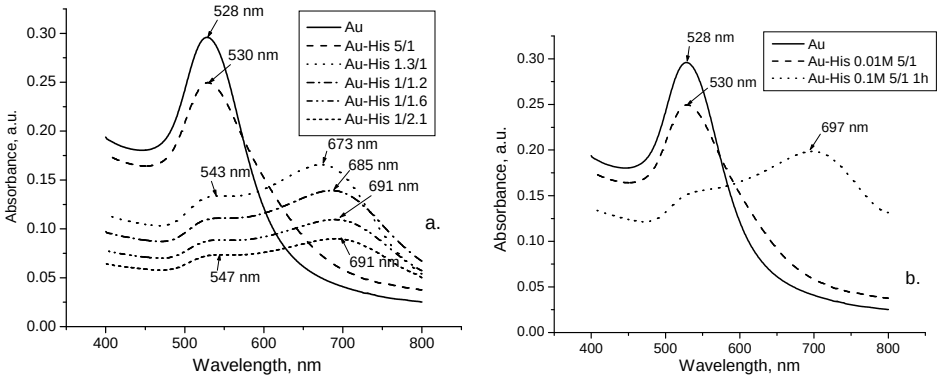

Fig.7. Optical spectrum of colloidal gold solution with 0.01 M histidine solution in different ratios (a) and with histidine solutions of different concentrations (b)

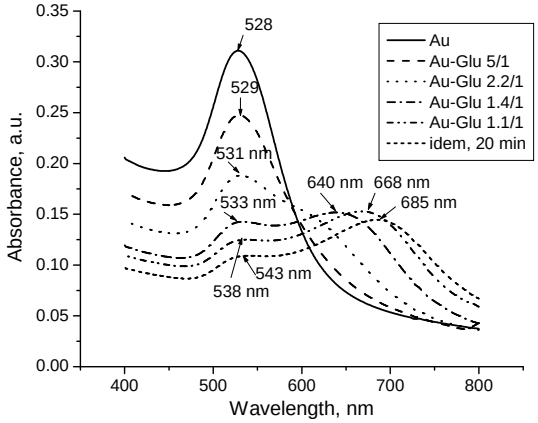

Fig.8. Optical spectrum of colloidal gold solution with 0.1 M glutamic acid solution in different ratios

Glutamic acid in a 0.1 M solution also initiates the aggregation of gold nanoparticles and the effect is increasing in time (Fig.8). It is interesting to mention that aspartic acid, closely related to glutamic acid, was used in the

reduction of chloroaurate ions and it was shown that this acid was strongly bonded to the nanoparticle surface and stabilized them efficiently [16].

Cysteine has the strongest effect from all the investigated amino acid solutions. Already a 10^{-3} M solution (Fig. 9a) added to the colloidal gold solution leads to a rapid aggregation, the peak for the broad band at longer wavelength surpasses rapidly the peak of the initial non-aggregated gold particles and the maximum wavelength goes above 700 nm. The 0.1 M cysteine solution (Fig. 9b) leads to the color change in blue of the gold solution at the first amount added. From Fig. 9b is also evident the time evolution of aggregation.

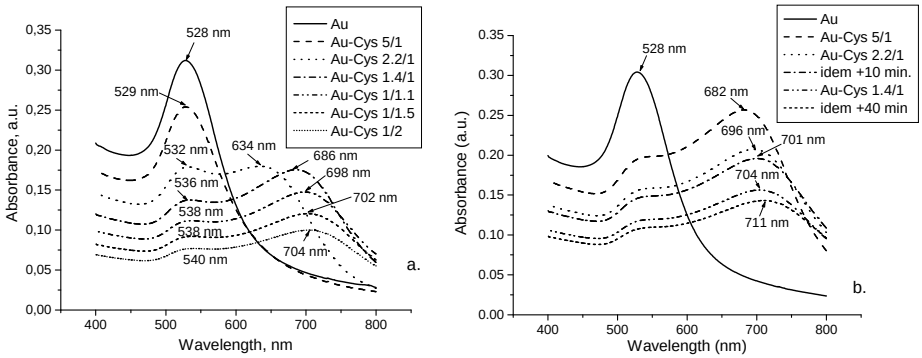

Fig.9. Optical spectrum of colloidal gold solution with 0.001 M (a) and 0.1 M (b) cysteine solution in different ratios.

These results support the observations about the interaction of cysteine with gold nanoparticles [19]; based on the analysis of FT-IR and Raman spectra, the authors affirm the existence of covalent interaction of sulphur and gold. The formation of a covalent bond Au-S is also assumed by other authors [21, 41]. It was suggested [38] that the positively charged amine group in cysteine ($-NH_3^+$) should interact with the negative charge on the surface of other gold nanoparticles through electrostatic binding, thus forming assemblies.

The band broadening and the shift of the surface plasmon band was shown to reflect the advanced aggregation of gold nanoparticles with decrease in pH and increase in electrolyte concentration [19].

The band broadening and the shift of the surface plasmon band was shown to reflect the advanced aggregation of gold nanoparticles with decrease in pH and increase in electrolyte concentration [19].

Further, we studied also the effect of two peptides on colloidal gold solutions. The dipeptide *glycil-glycine* (GlyGly) was added as a 0.4 M aqueous solution to the colloidal gold solution. The UV-Vis spectra are shown in Fig. 10 for the wavelengths range 250-800 nm (a) and 400-800 nm (b). The dipeptide solutions present an increased absorbance toward

lower wavelengths, with a shoulder at about 320 nm. For this reason, unlike the other investigated systems, here the absorbance does not decrease continuously with diminishing of gold content and the absorption maximum is shifted towards lower wavelengths. The absorption band of gold nanoparticles is not affected and no aggregation takes place.

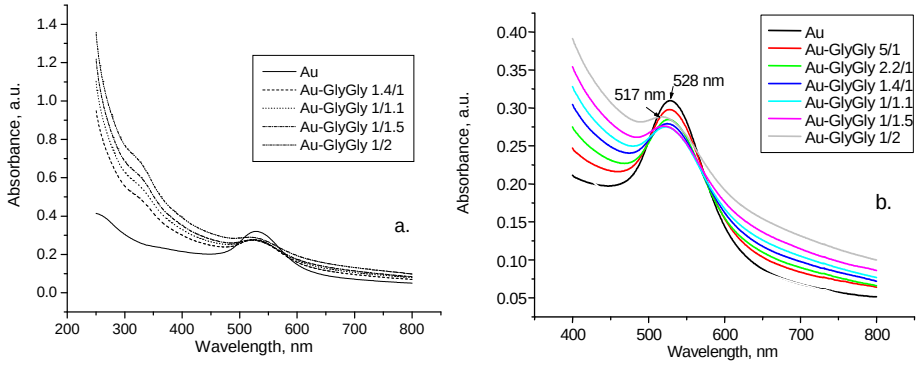

Fig.10. Optical spectrum of colloidal gold solution with 0.42 M glycyl-glycine (GlyGly) solution

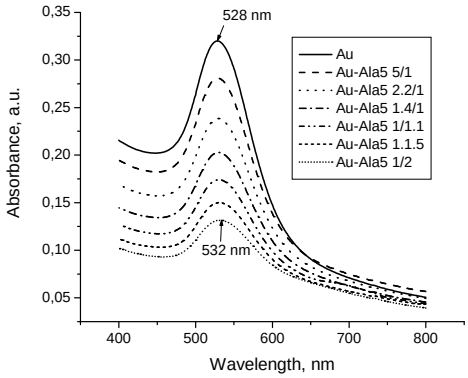

Fig.10c. Optical spectrum of colloidal gold solution with 0.007 M pentapeptide (Ala5) solution.

Similarly, a pentapeptide, *alanyl-alanyl-alanyl-alanyl-alanine* (Ala5) seems to have little effect on the gold nanoparticles (Fig. 10c); the plots are similar to those in Fig. 3.

The binding of amino acids with the gold nanoparticle interface may be achieved through the amine function. The binding could occur through the electrostatic interaction of the protonated amine group ($-NH_3^+$) with the surface bonded negatively charged citrate anions. On the other hand, a direct bonding of the amine group to the gold surface can not be excluded.

TEM images for gold nanoparticles with an 0.001 M cysteine solution show mostly linearly arranged assemblies of nanoparticles (Fig. 11), while for the nanoparticles with a 0.1 M lysine solution (Fig.12) and a 0.01 M arginine solution (Fig. 13) the assemblies are more complex.

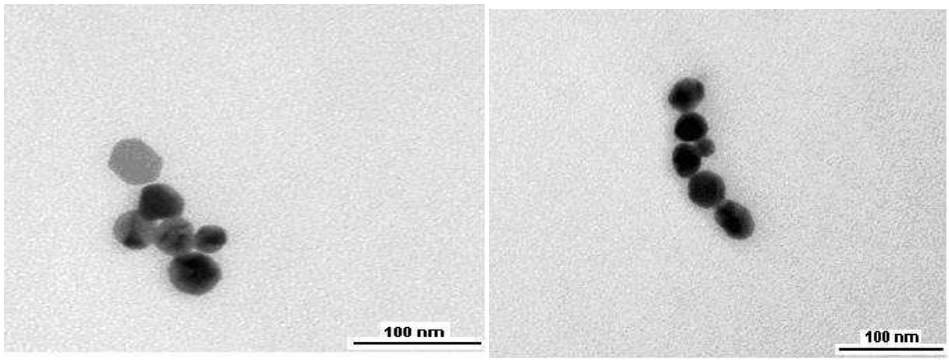

Fig. 11. TEM images of gold nanoparticles functionalized with 0.001 M cysteine solution

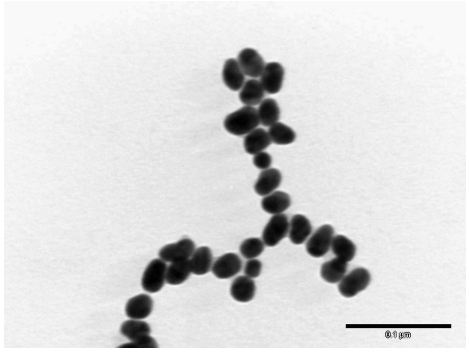

Fig.12. TEM image of gold nanoparticles capped with lysine (0.1 M), Au:Lys 1:1 ratio.

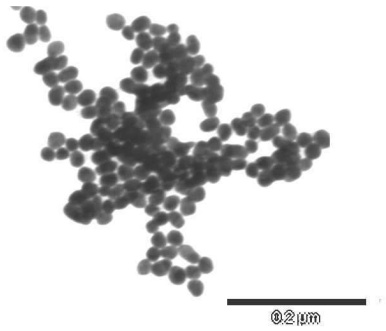

Fig. 13. TEM image of gold nanoparticles capped with arginine (0.01M), Au:Arg (1:1).

AFM images for assembled gold nanoparticles are shown in Fig. 14 with cysteine, in Fig. 15 with arginine, and in Fig. 16 with lysine. The atomic force microscope allows simultaneous acquisition of multiple images, such as topography and phase images, under tapping mode operation. The assembly of gold nanoparticles, mediated by the amino acid was deposited on planar hydrophobic glass or positively charged glass surfaces. Then, the assembly was observed by AFM under tapping mode and the structural features are visualized in Figs. 14-16. For instance the two-dimensional topographic image for lysine mediated gold nanoparticles assemblies (Fig. 16a) shows the

morphology of an almost ordered structure within domains, with small defects at domain boundaries. For the assembly of gold nanoparticles mediated by lysine,

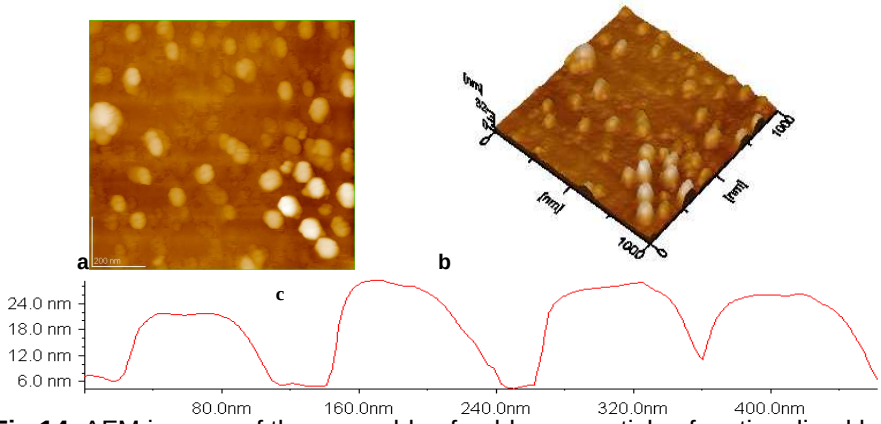

Fig.14. AFM images of the assembly of gold nanoparticles functionalized by cysteine. Scanned areas 1 x 1 μm^2. 2D-topography (a); 3D-view (b); cross section profile (c) along the arrow in panel a.

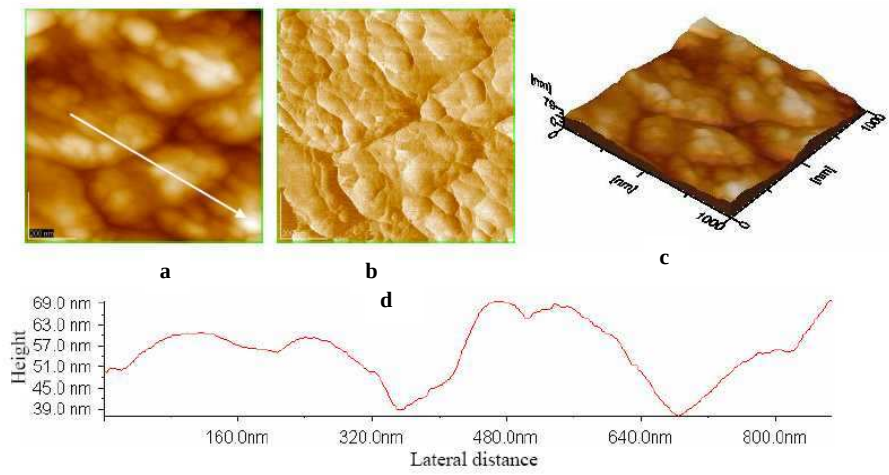

Fig. 15. AFM images of the assembly of gold nanoparticles functionalized by arginine. Scanned area 1 x 1 μm^2.; 2D-topography (a); phase image (b); 3D-view (c); cross section profile (d) along the arrow in panel a.

immobilized on glass surface, individual gold nanoparticles are visible from 2D-topography (Fig. 16a) and 3D-view (Fig. 16c). The phase image (Fig. 16b) shows also that the assembly of gold nanoparticles mediated by lysine is almost compact. All AFM images were acquired with high resolution as described elsewhere [44].

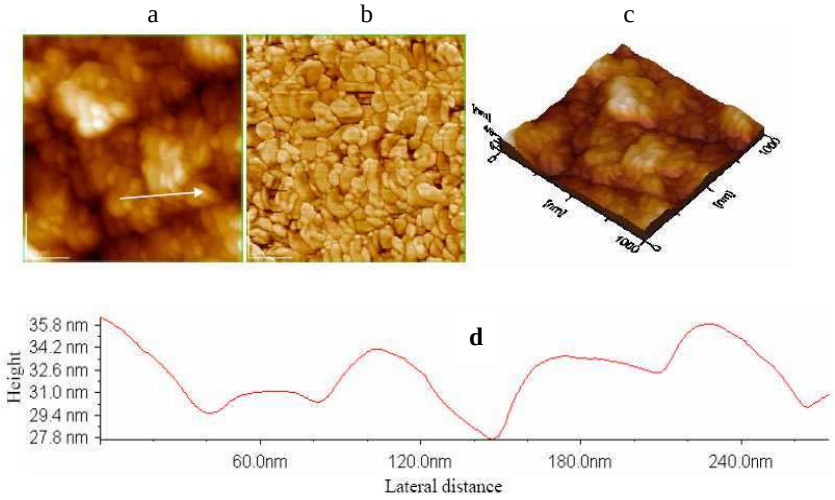

Fig.16. AFM images of the assembly of gold nanoparticles functionalized by lysine. Scanned area: 1 x 1 μm^2. 2D-topographic (a) and phase (b) and 3D-view (c); (d) cross section profile along the arrow in panel a.

The AFM images (Figs. 14-16) evidence the organization of gold nanoparticles functionalized with cysteine, arginine and lysine, respetively, within an almost compact network of aggregates, in substantial agreement with the UV-Vis spectroscopy. Also, the gold nanoparticles appear almost ordered both in AFM images and in cross section profile in substantial agreement with TEM images. For example, with cysteine (Fig. 14) it is observed a tendency of linear arrangements, in good agreement with TEM observations (Fig. 11).

In order to rationalize the behavior of the investigated amino acids versus gold nanoparticles we use a Venn diagram (Fig. 17), grouping amino acids according to their properties [45, 46]. The amino acids found to interact strongly with the gold nanoparticles and to initiate their aggregation were noted with "+", and those which give only slight shifts of the UV-Vis absorption band with "-". Most of the amino acids involved in the aggregation of gold nanoparticles fall in the class of "polar" amino acids, defined as those with side-chains that prefer to reside in an aqueous environment. For this reason, one generally finds these amino acids exposed on the surface of a protein [46]. All the "charged" amino acids present such strong interactions: both the amino acids that are usually *positive* (protonated) at physiological pH: lysine (K), arginine (R) and histidine (H), and those that are usualy *negative* (i.e. de-protonated) at

physiological pH: glutamic acid (E) and aspartic acid (D). The last one was reported to bind also strongly to the gold nanoparticles [5]. Cysteine (C) is probably bonded to the gold nanoparticles by its thiol (-SH) group, as was

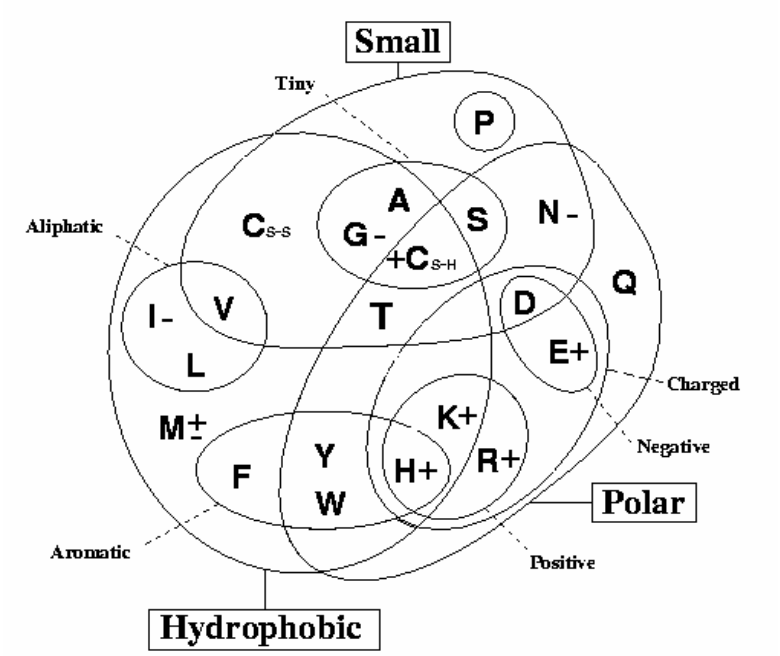

Fig. 17. Venn diagram grouping amino acids according to their properties (adapted from [45]) A – Alanine C_{S-H} – Cysteine C_{S-S} cystine D – Aspartic acid E – Glutamic acid F – Phenilalanine G – Glycine H – Histidine I – Isoleucine K – Lysine L – Leucine M – Methionine N – Asparagine P – Proline Q – Glutamine R – Arginine S – Serine T – Threonine V – Valine W – Triptophan Y - Tirosine

suggested by the study of ^{1}H NMR spectra [19,20]. All these amino acids, after their adsorption on the gold particles, have still two functional groups free to form bonds between particles. A possible mechanism of amino acid bindings to gold nanoparticles and the formation of particle aggregates are shown for cysteine in Fig.18. Methionine was labeled as "±" in the Venn diagram because it leads to aggregation only in time (Fig.4). The S-atom seems to be responsible for this activity. Glycine (G), isoleucine (I) and probably alanine (A), having only two functional groups, are probably only adsorbed on the gold nanoparticles (by the amino group) and stabilize these gold nanoparticles. Asparagine (N), having one –COOH group blocked by formation of the amide group ($CONH_2$) has a similar behavior as the last ones.

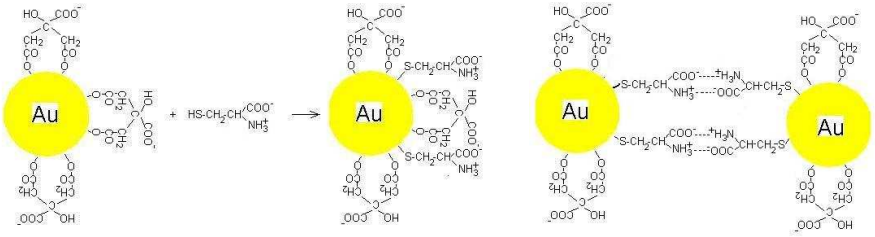

a b

Fig. 18. A model of cysteine binding to citrate capped gold nanoparticles (a) and of bonds formation between gold nanoparticles (b)

CONCLUSIONS

These data indicate that the binding of amino acids to the gold nanoparticles can lead to the self-assemblies almost well organized, particularly for amino acids possessing additional functional groups, such as amine, imidazole, thiol or thioeter besides the alpha-amine. The correlation between physical and chemical properties of amino acids, such as hydrophobicity and, acidity or basicity in various protolytic equilibria, and their molecular structure is in substantial agreement with their assembly effect on the gold nanoparticles. This effect could be explained primarily through the zwitterion-type electrostatic interactions between the charged amine and acid groups of the tested amino acid adsorbed/bound to different gold nanoparticles.

The affinity of gold nanoparticles towards amino acids can also lead to the development of new detection methods for analytical purposes, medical diagnostics and biosensors and to potential controlled drug delivery applications. On the other hand, the use of amino acids both in the functionalization of gold nanoparticles and in the cross-linking of amino acid capped gold nanoparticles leading to stable self-assemblies are promising ways to the synthesis of nanostructured biomaterials. The stabilization of gold nanoparticles through amino acids is also important for the understanding of complex phenomena involved in the formation of new biomaterials by binding of proteins with gold nanoparticles with important implications in nanoscience and nanotechnology. Another interesting possibility is covalent cross-linking of amino-acid capped nanoparticles by formation of amide bonds across nanoparticles. These types of studies are in progress in our laboratories.

ACKNOWLEDGEMENT

This research was financially supported by the Romanian Ministry of Education and Research (Scientific research project no.5/2005, within the Excellency Research Program).

REFERENCES

1. M.Zheng, X.Huang, In: *Biofunctionalization of Nanomaterials*, C.S.S.R. Kumar editor, Wiley-VCH, **2005**, 99-124
2. D.Fitzmaurice, S. Connolly, *Adv. Mater*., **1999**, *11*, 1202-1205
3. S.Mann, W.Shenton, M.Li, S. Connolly, D.Fitzmaurice, *Adv. Mater*., **2000**, *12*, 147-150
4. M.C. Daniel, D. Astruc, *Chem. Rev.* **2004,** *104,* 293-346
5. N.L. Rosi, C.A.Mirkin, *Chem.Rev.*, **2005**, *105*, 1547-1562
6. J.C.Love, L.A.Estroff, J.K.Knebel, R.G.Nuzzo, G.M.Whitesides, *Chem.Rev.*, **2005**, *105*, 1103-1170
7. G.M.Coppola, H.F.Schuster, *Asymmetric Synthesis. Construction of Chiral Molecules Using Amino Acids*, Wiley, New York, **1987**
8. C.C.You, M.De, G.Han, V.M.Rotello, *J. Am. Chem. Soc.,* **2005**, *127*, 12873-12881; C.C.You, M.De, V.M.Rotello, *Org.Lett.*, **2005**, *7*, 5685-5688
9. R.Levy, C.Doty, In: *Biofunctionalization of Nanomaterials*, C.S.S.R. Kumar editor, Wiley-VCH, **2005**, 235-269
10. J.Zsang, Q.Chi, J.U.Nielsen, E.P.Friis, J.E.T.Andersen, J.Ulstrup, *Langmuir*, **2000**, *16*, 7229-7237
11. S.Mandal, S.Phadtare, M.Sastry, *Curr. Appl. Phys.,* **2005**, *4*, 118-127
12. P.R. Selvakannan, S..Mandal, S.Phadtare, R.Pasricha, M. Sastry, *Langmuir*, **2003**, *19*, 3545-3549
13. H.Joshi, P.S.Shirude, V.Bansal, K.N.Ganeshand M. Sastry, *J. Phys. Chem. B*, **2004**, *108*, 11535-11540
14. Y. Shao, Y. Jin, S. Dong, *Chem. Commun.*, **2004**, 1104
15. P. Selvakannan, S.Mandal, S.Phadtare, A.Gole, R.Pasricha, S.D.Adyanthaya, M. Sastry, *J.Colloid Interf. Sci.*, **2004**, *269*, 97-102
16. S.Mandal, P.Selvakannan, S.Phadtare, R.Pasricha, M.Sastry, *Proc.Indian Acad.Sci. (Chem.Sci.)*, **2002**, *114*, 513-520
17. S.K.Bhargava, J.M.Booth, S.Agrawal, P.Coloe, G.Kar, *Langmuir*, **2005**, *32*, 5949-5956
18. S. Aryal, B.K. Remant, B. Narayan, C.K. Kim, HG.Y. Kim, *J. Colloid Interf.Sci.*, **2006**, *299*, 191-197
19. S.Aryal, K.C.Remant Bahadur, N.Dharmaraj, N.Bhattarai, C.H.Kim, H.Y.Kim, *Spectrochim. Acta*, *A*, **2006**, *63*, 160-163
20. S.Aryal, K.C.Remant Bahadur, N.Bhattarai, C.H.Kim, H.Y.Kim, *J.Colloid Interf. Sci.*, **2006**, *299*, 191-197
21. Z.P.Li, X.R.Duan, C.H.Liu, B.A.Du, *Anal. Biochem.*, **2006**, 351, 18-25
22. Y.F. Huang, Y.W. Lin, H.T. Chang, *Nanotechnology,* **2006,** *17***,** 4885-4894
23. R.Levy, N.T.K. Thanh, R. C. Doty, I. Hussain, R. J. Nichols, D. J. Schiffrin, M. Brust, D.G. Fernig, *J.Am.Chem.Soc.*, **2004**, *40*, 3685-3688
24. P.Tengvall, M.Lestelius, B.Liedberg, I.Lundstroem, *Langmuir*, **1992**, *8*, 1236-1238
25. Y.C.Sasaki, K.Yasuda, Y.Susuki, T.Ishibashi, I.Satoh, Y.Fujiki, S.Ishiwata, *Biophys. J.,* **1997**, *72*, 1842-1848

26. I.Willner.. E.Katz, B.Willner, R.Blonder, V.Heleg-Shabtai, A.F.Bückmann, , *Biosens. Bioelectron.,* **1997**, *12*, 337-356
27. O. Horovitz, Gh. Tomoaia, A. Mocanu, T. Yupsanis, Tomoaia-Cotisel, *Gold Bull.***, 2007,** *40,* 213-218
28. O. Horovitz, A. Mocanu, Gh. Tomoaia, L. Olenic, Gg. Mihăilescu, O. Boroştean, A. Popoviciu, C. Crăciun, T. Yupsanis, M.Tomoaia-Cotisel, In: "Convergence of micro-nano-biotechnologies", Series "Micro and Nanoengineering", Vol.9, Ed. Academiei, Bucureşti, **2006**, 133-147
29. E. Indrea, S. Dreve, I. Bratu, Gh. Mihailescu, L. Olenic, Gh. Tomoaia, A. Mocanu, O. Horovitz, M. Tomoaia-Cotisel, In "Technical Proceedings of the 2007 Nanotechnology Conference and Trade Show", NSTI-Nanotech, Santa Clara, **2007**, Vol. *4*, 461–464
30. O. Horovitz, A. Mocanu, Gh. Tomoaia, L. Bobos, D. Dubert, I. Dăian, T. Yupsanis, M. Tomoaia-Cotisel, *Studia Univ. Babes-Bolyai, Chem*., **2007**, *52* (1), 97-108
31. S.Chah, M.R.Hammond, R.N.Zare, *Chem. Biol.*, **2005**, *12*, 323-328
32. J. A. DeRose, R. M. Leblanc, *Surf. Sci. Rep.*, **1995,** *22,* 73-77 ; Y. F. Dufrene, G. U. Lee, *Biochim. Biophys. Acta*, **2000**, *1509*, 14-17
33. K. S. Birdi, *Scanning Probe Microscopes. Applications in Science and Technology*, CRC Press, New York, **2003**
34. M. Tomoaia-Cotisel, Gh. Tomoaia**,** V. D. Pop, A. Mocanu, G.Cozar, N. Apetroaei and Gh. Popa, *Rev. Roum. Chim.,* **2005***, 50*, 471-478
35. N.R.Jana, L.Gearheart, S.O.Obare, C.J.Murphy, *Langmuir*, **2002**, *18*, 922-927
36. K.S.Mayya, V.Patil, M.Sastry, *Langmuir*, **1997**, *13*, 3944-3947
37. J.J.Storhoff, R.Elghanian, R.C.Mucic, C.A.Mirkin, R.L.Letsinger, *J.Am.Chem.Soc.*, **1998**, *120*, 1959-1964
38. U.Kreibig, L.Genzel, *Surface Sci.,* **1985**, *156*, 678-700
39. C.A.Mirkin, R.L.Letsinger, R.C.Mucic, J.J.Storhoff, *Nature*, **1996**, *382*, 607-609
40. L. Xu, Y. Guo, R. Xie, J. Zhuang, W. Yang, *Nanotechnology*, **2002**, *13*, 725-728
41. P.K.Sudeep, S.T.S. Joseph, K.G.Thomas, *J. Am. Chem. Soc.*, **2002**, *127*, 6516-6517
42. I.S.Lim, W.Ip, E.Crew, P.N.Njoki, D.Mou, C.J. Zhong, Y.Pan, S.Zhou, *Langmuir*, **2007**, *23*, 826-833
43. C.Ku, Y.Zu, V.Wimg-WahYam, *Anal.Chem.* **2007**, *79*, 666-572
44. M. Tomoaia-Cotisel, In: "Convergence of Micro-Nano-Biotechnologies", Series "Micro and Nanoengineering", Vol.9, Ed.Academiei, **2006**, 147 - 161
45. C.D. Livingstone, G.J.Barton, *Comput. Appl. Biosci.*, **1993,** *9*, 745-756
46. M.J. Betts, R.B. Russell. In „*Bioinformatics for Geneticists*", M.R. Barnes and I.C. Gray eds, Wiley, **2003**